Structure of Chaos in the Laser with Saturable Absorber

F. Papoff,[1] A. Fioretti,[2] E. Arimondo,[2] G. B. Mindlin,[3],[a] H. Solari,[3],[b] and R. Gilmore[3]

[1]*Scuola Normale Superiore, Piazza dei Cavalieri 2, 56100 Pisa, Italy*

[2]*Dipartimento di Fisica, Piazza Torricelli 6 56100 Pisa, Italy*

[3]*Department of Physics and Atmospheric Science, Drexel University, Philadelphia, Pennsylvania 19104*

(Received 7 August 1991)

We carry out a topological analysis on an experimental data set from the laser with saturable absorber. This analysis is based on the topological organization of low period orbits extracted from chaotic time series data. This allows us to determine for the first time that previously proposed models are compatible with the data.

PACS numbers: 42.50.Lc, 05.45.+b, 42.55.−f

It has recently become possible to provide a topological classification of strange attractors. In this classification scheme the topological structure of a strange attractor is given by a set of integers. These integers describe the structure of the "knot-holder" [1] or "template" which supports the strange attractor [2]. The template describes the stretching and compressing mechanisms responsible for creating the strange attractor. These stretching and compressing mechanisms are also responsible for organizing the unstable periodic orbits which are embedded in the strange attractor in a unique way.

This topological classification is in contrast to the classification of strange attractors according to their metric properties (e.g., Lyapunov exponents, various dimensions). Metric properties are invariant under a coordinate transformation but not under control parameter variation. Topological properties remain invariant under both coordinate transformations and control parameter variations, or change in experimental conditions. This means, in particular, that chaotic data sets taken for a physical system under different experimental conditions will exhibit the same topological classification.

Furthermore, it is possible to determine the topological classification of a strange attractor by carrying out an analysis ("topological analysis") on scalar time series data [3]. This provides, for the first time, a test to determine whether a model which is proposed to describe a chaotic process is in fact compatible with that process. Topological analyses are carried out on the experimental time series data and data generated by the model. If the topological analyses identify different templates (sets of integers), the model can be rejected as not compatible with the data. Otherwise, the model is compatible with the data.

In this Letter we apply this topological analysis, for the first time, to determine whether models proposed to described the laser with saturable absorber (LSA) [4–7] are compatible with a number of experimental data sets which have been taken from the LSA [6–9].

The experimental setup consists of an infrared cavity containing a discharge CO_2 amplifier and an absorber cell. We have used CH_3I:He and OsO_4:He in the ratio 1:20 as absorbers. The laser output intensity I is digitized and discretely sampled at a rate of about 80 samples per period for fixed values of the control parameters. These include the discharge current, the absorber pressure, and the laser frequency detuning. A number of long time series, up to 32×10^3 8-bit data, were stored in a microcomputer by use of a digital oscilloscope.

In the region of the LSA where instabilities and chaos are found, the laser intensity pulse starts below threshold, developing a large peak L followed by a variable number of small peaks S. Each minimum is followed by a maximum; the deeper the minimum, the more intense the following maximum. A segment of a typical data set is shown in Fig. 1.

Three [4,6], four [5], and five [7] variable models have been proposed to describe the LSA. The mechanism responsible for the existence of chaotic behavior in these models is the following. An unstable limit cycle (saddle cycle) or its degenerate limit, an unstable focus, has stable and unstable invariant manifolds which approach tangency [10] [cf. Fig. 2(a)]. In the three-, four-, and five-dimensional models the unstable manifold of the saddle cycle is two dimensional, while the stable manifold is 2D, 3D, and 4D, respectively. As the tangency is approached, a number of stable periodic orbits are created by saddle-node bifurcations, which then undergo period-doubling cascades. This generates a complicated dynamics even before the tangency occurs [10,11]. When the manifolds behave as shown in Fig. 2(b) the flow is hyperbolic and exhibits a Smale horseshoe [10] with zero global torsion. A point in the strange attractor near the unstable invariant manifold W^u will evolve during one period along W^u (stretching) while at the same time being compressed along the direction of the stable manifold W^s towards the invariant set W^u (folding). The stretching and folding mechanisms, responsible for the creation of chaos, are represented schematically by the template for this flow, shown in Fig. 2(c).

To determine whether these models are compatible with the experimental data, we must identify the template underlying the experimental strange attractor, and compare it with the template shown in Fig. 2(c). The topological analysis of the chaotic data was carried out in a number of simple steps.

First, the unstable periodic orbits embedded in the strange attractor were determined by the method of close

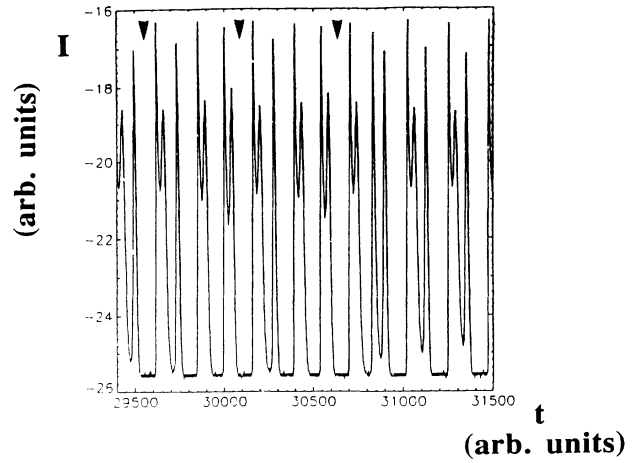

FIG. 1. A segment of the time series data. The intensity is plotted vs time. In this case a close return after 7 periods occurs (indicated by the arrows), as the strange attractor is closely following a period-7 orbit, staying close to it during approximately 14 periods.

returns [3]. If the phase-space trajectory of the system enters the neighborhood of an unstable periodic orbit with a relatively small Lyapunov exponent, it may remain in the neighborhood of that orbit sufficiently long so that it returns near its starting point and evolves near an earlier point of its trajectory (cf. Fig. 1). Such close return segments are easily identified by plotting $|I(i)-I(i+p)|$, where i indexes the discretely sampled intensity ($1 \leq i \leq 32\times10^3$). Segments $i_{\min} < i < i_{\max}$ where the difference above is relatively small indicate segments of chaotic time series data that can then be used as representations of unstable periodic orbits of period p, measured in units of the sample rate. In this way, four or more periodic orbits were located in each data file taken under different experimental conditions for the LSA.

Second, an embedding of these segments as well as the entire strange attractor in R^3 must be constructed so that topological organization of orbit pairs can be determined. We have adopted a differential phase-space embedding

$$I(i) \rightarrow [y_1(i), y_2(i), y_3(i)],$$

where $y_1(i) = \sum_{j=1}^{i} I(j) e^{-(i-j)/N}$, $y_2(i) = I(i)$, $y_3(i) = I(i) - I(i-1)$. Here N is taken as about two cycle times ($N \sim 2\times80$) [3]. This embedding of the period-1 and -3 orbits is shown in Fig. 3.

The embedded strange attractor had a hole in the center, making possible the construction of a Poincaré section. In each section we were able to construct a return map. For each map we found an orientation-preserving and an orientation-reversing branch. This allowed the development of a symbolic dynamics for all orbits in each data set: x (y) for passage through the orientation-preserving (-reversing) branch. A segment of data which closely follows the unstable period-1 orbit (y) is shown in Fig. 4. This clearly identifies the orbit y as a

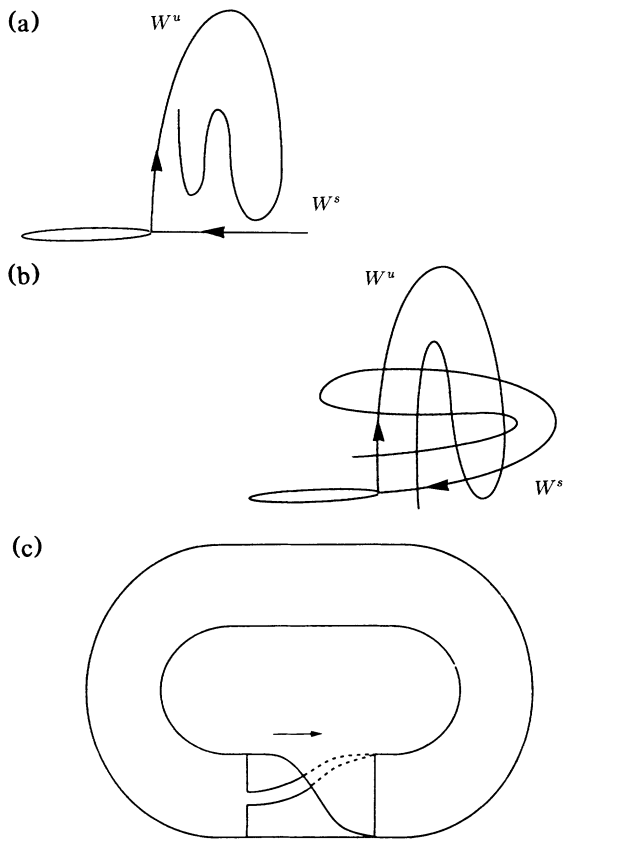

FIG. 2. (a) A saddle cycle whose unstable and stable manifolds are approaching a tangency. (b) The stable and unstable manifolds of a saddle cycle after the last tangency. There is a hyperbolic invariant set coexisting with the saddle cycle. (c) The horseshoe template. For each periodic orbit held by this manifold, there is an orbit in the invariant set of (b) with identical topological properties.

flip saddle, as the orbit segment yy forms the boundary of a nonorientable strip. This allows the identification x with the small peaks, $x \sim S$, and y with the large peaks, $y \sim L$. The unstable limit cycle y describes unstable periodic behavior of the LSA consisting of a series of large peaks.

Third, the linking numbers of all pairs of periodic orbits identified in each data set were determined [3,12]. The linking number of two orbits is defined by a Gauss integral [3] and is roughly the number of times the two orbits wind around each other. Computation of the linking number in the differential phase-space embedding is particularly easy and was done by counting crossings of the orbits. This is shown in Fig. 3, where the over and under crossings of the period-1 and period-3 orbits are clearly indicated.

Fourth, a template was identified on the basis of the linking numbers of a small set of orbits. Each template has a unique signature in terms of the linking numbers of pairs of periodic orbits. In fact, the linking numbers of

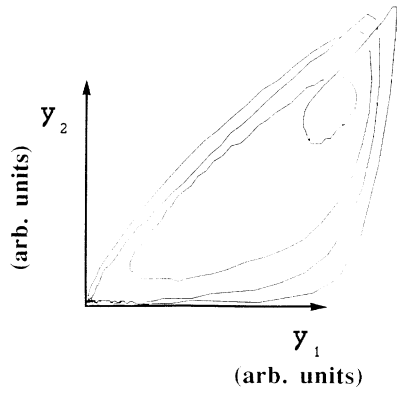

FIG. 3. A two-dimensional projection of the three-dimensional embedding for the segment close to the period-1 orbit and for a segment close to a period-3 orbit. The over and under crossings keep track of the third dimension. The segments of orbits in the outer part of the figure have higher values of the third coordinate than the segments of orbits in the inner part. Two orbit segments which cross each other are interchanging their order on the third coordinate and, for this reason, are on the orientation reversing branch. The period-1 and period-3 orbits cross each other 4 times, so their linking number is $\frac{1}{2}(4)=2$.

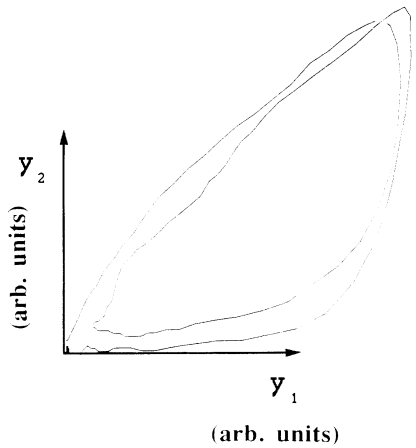

FIG. 4. Two cycles around the period-1 flip saddle orbit. As in Fig. 3, the segments of orbits in the outer part of the figure have higher values of the third coordinate than the segments in the inner part. The strip whose boundary is approximated by these orbits is nonorientable as it is a rectangle with two sides joined with a half twist.

only the period-1 and period-2 orbits suffice to distinguish different templates. When not all of these orbits can be extracted from the data, alternative subsets of orbits can be used to identify the template. Additional orbits then provide confirmation of the template identification [3].

For each of the experimental LSA data files studied, a minimum of four periodic orbits was reconstructed. These orbits had symbolic names, y, yx^n, $yx^{n-1}y$, with n ranging from 1 to 15. Orbits of higher period, which are compositions of different pulses with $n=1,2$ have also been extracted from some files. For each of the files studied, the template identified was the horseshoe template with zero global torsion. In every case, the template was overdetermined by the periodic orbits extracted.

We point out here that we cannot entirely reconstruct the phase space, since the intensity of the LSA goes below our detection limit between most successive pulses. Thus, in principle we cannot exclude the possibility that part of the large peaks which are not completely reconstructed lie on a third branch of a template. However, all the orbits extracted from our data set are compatible with a template having only two branches, which is the simplest template compatible with the data.

This analysis reveals that as the control parameters in the experiments are changed, the template supporting the strange attractor remains unchanged. What does change is the set of unstable periodic orbits which are present in the strange attractor and/or their degree of instability. These changes have consequences which can be easily visualized. This can be done by plotting the cumulative number of times the phase-space trajectory passes through the orientation-preserving (or -reversing) branch of the template (p_0 or p_1) as a function of the cumulative number of passes through the template (p_0+p_1). For each of the files studied, this plot was nearly a straight line, with slope P/Q. For each of the files, the higher period orbits extracted had a "rotation number" $p_1/(p_0+p_1)$, well approximated by the ratio P/Q. In Fig. 5 we show such a plot for three LSA data files taken at different control parameter values.

One of the benefits of a topological analysis is that the recovery of a "badly ordered" or non-well-ordered orbit from the data set is a sufficient condition to show that the topological entropy of the flow is positive, and that the temporal behavior is chaotic [13]. This requires much less work than an analysis based on the computation of Lyapunov exponents, which can be problematic for relatively small data sets. We have found different badly ordered orbits in LSA data files. One of these orbits of period 7 ($yxyyxyx$) is shown in Fig. 1.

In conclusion, for the first time a topological analysis of chaotic time series data was used to determine if models proposed to describe the dynamics of a physical system are in fact compatible with the dynamics responsible for generating the data. The large number of experimental data sets which were recorded and analyzed for the LSA indicate that the dynamics is governed by a flow organized by a Smale horseshoe with zero global torsion. Variation of the control parameters restricts the flow to different parts of the underlying template, which remains unchanged as the control parameters are varied. Previously proposed models of dimensions three, four, and five

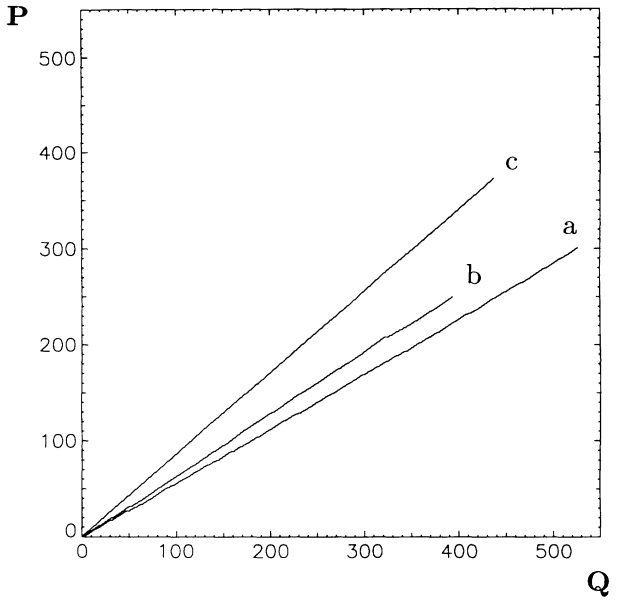

FIG. 5. Cumulative number of passes P through the orientation reversing branch vs the cumulative number of passes Q through the template for three different control parameter values. (Curve a) Absorber CH_3I:He with amplifier current discharge of 10.9 mA and pressure 0.1 mbar; (curves b and c) absorber OsO_4:He with amplifier current discharge of 9.3 mA and pressure 0.73 and 0.47 mbar, respectively.

exhibit the same underlying template, and are therefore not inconsistent with the experimental data sets.

This work was partially performed during the visit of one author (F.P.) to Drexel University. We wish to thank Professor J. R. Tredicce for helpful discussions and Dr. M. A. Natiello for help in the preparation of the computer codes. One of us (F.P.) thanks Foundazione A. Della Riccia for financial support. This work was partially supported by NSF Grant No. PHY88-43235.

[a]Present address: Departamento de Física y Matematica Aplicada, Facultad de Ciencias, Universidad de Navarra, 31080 Pamplona, Navarra, Spain.

[b]Present address: Departamento de Física, FCEN-Universidad de Buenos Aires, Pabellón I, Ciudad Universitaria, 1428 Buenos Aires, Argentina.

[1] P. Holmes, in *New Directions in Dynamical Systems*, edited by T. Bedford and J. Swift (Cambridge Univ. Press, Cambridge, 1988), p. 150.

[2] G. B. Mindlin, X. J. Hou, H. G. Solari, R. Gilmore, and N. B. Tufillaro, Phys. Rev. Lett. **64**, 2350 (1990).

[3] G. B. Mindlin, H. G. Solari, M. A. Natiello, R. Gilmore, and X. J. Hou, J. Nonlinear Sci. **1**, 147 (1991).

[4] B. Zambon, Phys. Rev. A **44**, R688 (1991).

[5] F. L. Hong, M. Tachikawa, T. Oda, and T. Shimizu, J. Opt. Soc. Am. B **6**, 1378 (1989).

[6] M. Lefranc, D. Hennequin, and D. Dangoisse, J. Opt. Soc. Am. B (to be published).

[7] D. Hennequin, F. de Tomasi, B. Zambon, and E. Arimondo, Phys. Rev. A **37**, 2243 (1988).

[8] D. Dangoisse, A. Bekkali, F. Papoff, and P. Glorieux, Europhys. Lett. **6**, 335 (1988).

[9] M. Tachikawa, F. L. Hong, K. Tanii, and T. Shimizu, Phys. Rev. Lett. **60**, 2266 (1988); **61**, 1042 (1988).

[10] J. Guckenheimer and P. Holmes, *Nonlinear Oscillations, Dynamical Systems, and Bifurcations of Vector Fields* (Springer-Verlag, New York, 1983).

[11] F. Papoff, A. Fioretti, and E. Arimondo, Phys. Rev. A **44**, 4639 (1991).

[12] L. H. Kaufman, *On Knots* (Princeton Univ. Press, Princeton, NJ, 1987).

[13] J. M. Gambaudo, S. Van Strien, and C. Tresser, Ann. Inst. Henri Poincaré **49**, 335 (1989).